

A study of chiral symmetry in quenched QCD using the Overlap-Dirac operator

Robert G. Edwards, Urs M. Heller, Rajamani Narayanan

SCRI, Florida State University, Tallahassee, FL 32306-4130, USA

e-mail: {edwards,heller,rmaray}@scri.fsu.edu

We compute fermionic observables relevant to the study of chiral symmetry in quenched QCD using the Overlap-Dirac operator for a wide range of the fermion mass. We use analytical results to disentangle the contribution from exact zero modes and simplify our numerical computations. Details concerning the numerical implementation of the Overlap-Dirac operator are presented.

I. INTRODUCTION

The Overlap-Dirac operator [1] derived from the overlap formalism for chiral fermions on the lattice [2] provides a non-perturbative regularization of chiral fermions coupled vectorially to a gauge field. The massless Overlap-Dirac operator is given by (the lattice spacing is set to one)

$$D(0) = \frac{1}{2} [1 + \gamma_5 \hat{H}_a]. \quad (1)$$

\hat{H}_a is a hermitian operator that depends on the background gauge field and has eigenvalues equal to ± 1 . There are two sets of choices for \hat{H}_a . The simplest example in the first set is $\epsilon(H_w)$ where $\gamma_5 H_w(-m)$ ($m_c < m < 2$) is the usual Wilson-Dirac operator on the lattice

with a negative fermion mass [1] and $-m_c$ is the critical mass, which goes to zero in the continuum limit. One could replace H_w by any improvements of the Wilson-Dirac operator with the mass in the supercritical region but smaller than where the doublers become light. The simplest example in the other set is obtained from the domain wall formalism [3] and $\hat{H}_a = \epsilon(\log(T_w))$ where $T_w(m)$ is the transfer matrix associated with the propagation of the four dimensional Wilson fermion in the extra direction [4]. Here $m_c < m < 2$ is the domain wall mass. Again, one can replace the five dimensional Wilson-Dirac fermion by any improvements. The massive Overlap-Dirac operator is given by

$$D(\mu) = \frac{1}{2} [1 + \mu + (1 - \mu)\gamma_5 \hat{H}_a] \quad (2)$$

with $0 \leq \mu \leq 1$ describing fermions with positive mass all the way from zero to infinity. For small μ , μ is proportional to the fermion mass. When $\hat{H}_a = \epsilon(\log(T_w))$, the bare mass μ is exactly the standard mass term in the domain wall formalism [5,4]. The analytical expressions derived in this paper are valid for any generic choice of \hat{H}_a . Our numerical results are obtained with the choice of $\hat{H}_a = \epsilon(H_w)$.

The massless Overlap-Dirac operator has exact zero eigenvalues, due to topology, in topologically non-trivial gauge fields, and these zero eigenvalues are always paired with eigenvalues exactly equal to unity [1,6]. All exact zero eigenvalues are chiral, and their partners at unity are also chiral but with opposite chirality. The rest of the eigenvalues of the Overlap-Dirac operator come in complex conjugate pairs and one eigenvector is obtained by the operation of γ_5 on the other eigenvector. The behavior of the Overlap-Dirac operator on the lattice is essentially that of a continuum massless fermion.

The external fermion propagator is given by

$$\tilde{D}^{-1}(\mu) = (1 - \mu)^{-1} [D^{-1}(\mu) - 1] . \quad (3)$$

The subtraction at $\mu = 0$ is evident from the original overlap formalism [2] and the massless propagator anti-commutes with γ_5 [1,7]. With our choice of subtraction and overall normalization the propagator satisfies the relation

$$\mu \langle b^\dagger | [\gamma_5 \tilde{D}^{-1}(\mu)]^2 | b \rangle = \langle b^\dagger | \tilde{D}^{-1}(\mu) | b \rangle \quad \forall b \quad \text{satisfying} \quad \gamma_5 | b \rangle = \pm | b \rangle \quad (4)$$

for all values of μ in an arbitrary gauge field background. This relation will be evident from the discussion in section II. The fermion propagator on the lattice is related to the continuum propagator by

$$D_c^{-1}(m_q) = Z_\psi^{-1} \tilde{D}^{-1}(\mu) \quad \text{with} \quad m_q = Z_m^{-1} \mu \quad (5)$$

where Z_m and Z_ψ are the mass and wavefunction renormalizations, respectively. Requiring that (4) hold in the continuum, results in $Z_\psi Z_m = 1$. For $\hat{H}_a = \epsilon(H_w(m))$ we find

$$Z_\psi = Z_m^{-1} = 2m \quad (6)$$

at tree level, and a tadpole improved estimate gives

$$Z_\psi = Z_m^{-1} = \frac{2}{u_0} [m - 4(1 - u_0)] \quad , \quad (7)$$

where u_0 is one's favorite choice for the tadpole link value. Most consistently, for the above relation, it is obtained from m_c , the critical mass of usual Wilson fermion spectroscopy.

In this paper, we study QCD in the quenched limit on the lattice using the Overlap-Dirac operator. Our aim is to study the behavior of chiral susceptibilities on a finite lattice in the massless limit. In section II, we derive analytic expressions for various chiral susceptibilities using the spectral decomposition of the Overlap-Dirac operator. These formulae do not reveal any new physics not already known from formal arguments in the continuum; however, they are valid for any lattice spacing, not only in the continuum limit. These formulae will help us simplify the numerical computations and disentangle contributions due to global topology from the rest of the contributions. We also discuss the massless limit of the chiral susceptibilities in quenched QCD. In section III, we present some details of the algorithm used to numerically compute the chiral susceptibilities on a finite lattice. Our numerical results are presented in section IV and compared with the analytical expressions obtained in section II. Similar numerical work has been done recently using domain wall fermions with a finite extent in the fifth direction [8].

II. CHIRAL CONDENSATE AND SUSCEPTIBILITIES

An analysis of the Overlap-Dirac operator can be performed in an arbitrary gauge field background by noting that \hat{H}_a can be written in block diagonal form with 2×2 blocks in the chiral basis [6]. We start by recalling a few properties of the Overlap-Dirac operator D for a single Dirac fermion: $(\gamma_5 D)^2$ commutes with γ_5 and both operators can therefore be diagonalized simultaneously. The massive Overlap-Dirac operator can be related to the massless one, from (2), as

$$D(\mu) = (1 - \mu) \left[D(0) + \frac{\mu}{1 - \mu} \right] . \quad (8)$$

We find it convenient to work in the chiral eigenbasis of $(\gamma_5 D(0))^2$ for massless fermions, $\mu = 0$. In this basis $D(\mu)$ takes on the following block diagonal form [6]:

- There are $|Q|$ blocks of the form

$$\begin{pmatrix} \mu & 0 \\ 0 & 1 \end{pmatrix}$$

associated with the global topology of the configuration. These $|Q|$ blocks will be robust under perturbations of the gauge field background. The two modes per block have opposite chiralities. The chiralities of the modes with eigenvalues μ will all be the same and dictated by the sign of the global topology Q .

- There are $2NV - |Q|$ blocks of the form

$$\begin{pmatrix} (1 - \mu)\lambda_i^2 + \mu & (1 - \mu)\lambda_i\sqrt{1 - \lambda_i^2} \\ -(1 - \mu)\lambda_i\sqrt{1 - \lambda_i^2} & (1 - \mu)\lambda_i^2 + \mu \end{pmatrix}$$

with $0 \leq \lambda_i \leq 1$, $i = 1, 2, \dots, 2NV - |Q|$, depending on the background gauge field. The λ_i^2 's are the eigenvalues of $(\gamma_5 D(0))^2$. We leave open the possibility that n'_z of these eigenvalues could be exactly zero. These are accidental zeros in that they would

be lifted by a small perturbation of the gauge field background. In each subspace, $\gamma_5 = \begin{pmatrix} 1 & 0 \\ 0 & -1 \end{pmatrix}$.

The matrix can be inverted in the above form to give the following block diagonal form for the external propagator $\tilde{D}^{-1}(\mu) = (1 - \mu)^{-1} [D^{-1}(\mu) - 1]$:

- There are $|Q|$ blocks of the form

$$\begin{pmatrix} \frac{1}{\mu} & 0 \\ 0 & 0 \end{pmatrix}$$

- There are $2NV - |Q|$ blocks of the form

$$\frac{1}{\lambda_i^2(1 - \mu^2) + \mu^2} \begin{pmatrix} \mu(1 - \lambda_i^2) & -\lambda_i\sqrt{1 - \lambda_i^2} \\ \lambda_i\sqrt{1 - \lambda_i^2} & \mu(1 - \lambda_i^2) \end{pmatrix}$$

We will use $\langle \cdots \rangle_A$ to denote the expectation value of a fermionic observable in a fixed gauge field background, and $\langle \cdots \rangle$ for the expectation value averaged over a gauge field ensemble. From the above expression for the fermion propagator in a background gauge field, we obtain

$$\frac{1}{V} \sum_x \langle \bar{\psi}(x) \gamma_5 \psi(x) \rangle_A = \frac{1}{V} \text{Tr}[\gamma_5 \tilde{D}^{-1}] = \frac{Q}{\mu V} \quad (9)$$

in a gauge field background with global topology Q . Here Tr denotes a trace over space, color and Dirac indices. $\langle \bar{\psi} \gamma_5 \psi \rangle$ goes to zero when averaged over all gauge field configurations. We also find

$$\frac{1}{V} \sum_x \langle \bar{\psi}(x) \psi(x) \rangle_A = \frac{1}{V} \text{Tr}[\tilde{D}^{-1}] = \frac{|Q|}{\mu V} + \frac{1}{V} \sum_i \frac{2\mu(1 - \lambda_i^2)}{\lambda_i^2(1 - \mu^2) + \mu^2}. \quad (10)$$

To discuss the gauge field average of $\langle \bar{\psi} \psi \rangle$ in the massless limit, we have to distinguish four cases ¹:

- We consider full QCD with $n_f > 1$ flavors in a fixed finite volume. Gauge fields with non-zero topology are then suppressed by $\mu^{n_f |Q|}$, the contribution from the zero modes to $\det D(\mu)$. Accidental zero modes are also suppressed by the fermion determinant, by $\mu^{2n_f n'_z}$. Therefore, we find from eq. (10)

¹ We do not consider the case of one flavor QCD since the chiral symmetry is broken by the anomaly.

$$\frac{1}{V} \sum_x \langle \bar{\psi}(x) \psi(x) \rangle = \mathcal{O}(\mu) \quad (11)$$

and the chiral condensate vanishes in the massless limit in a finite volume.

- We consider full QCD with $n_f > 1$ flavors in the infinite volume limit, taking the volume to infinity before taking the mass to zero. In this limit we expect $\langle |Q| \rangle$ to be proportional to \sqrt{V} , and therefore the first term in (10) will go to zero in the infinite volume limit. The spectrum, λ_i , becomes continuous in the infinite volume limit, represented by a spectral density, $\rho(\lambda)$. Then we obtain,

$$\lim_{\mu \rightarrow 0} \lim_{V \rightarrow \infty} \frac{1}{V} \sum_x \langle \bar{\psi}(x) \psi(x) \rangle = \pi \rho(0) \quad (12)$$

and the chiral condensate is proportional to the spectral density at zero just as expected in the continuum [9].

- We consider a quenched theory in a fixed finite volume. Now, gauge field configurations with nontrivial topology and accidental zero modes are not suppressed by a fermion determinant, and we obtain

$$\lim_{\mu \rightarrow 0} \frac{1}{V} \sum_x \langle \bar{\psi}(x) \psi(x) \rangle = \lim_{\mu \rightarrow 0} \frac{\langle |Q| + 2n'_z \rangle}{\mu V} \quad (13)$$

$2n'_z$ is the number of accidental, paired zero modes. Since they are lifted by a small perturbation of the gauge fields, the gauge fields for which such accidental zero modes exist are probably of measure zero, and we expect $\langle n'_z \rangle = 0$. Thus in any finite volume $\langle \bar{\psi} \psi \rangle$ diverges like $\frac{1}{\mu}$ in the quenched theory with a coefficient equal to $\frac{\langle |Q| \rangle}{V}$. The expectation value here is over a pure gauge ensemble, and the coefficient is therefore expected to be proportional to $1/\sqrt{V}$.

- We consider a quenched theory in the infinite volume limit, taking the volume to infinity before taking the mass to zero. Then, the first term in (10) vanishes and from the second we obtain

$$\lim_{\mu \rightarrow 0} \lim_{V \rightarrow \infty} \frac{1}{V} \sum_x \langle \bar{\psi}(x) \psi(x) \rangle = \pi \rho(0) \quad (14)$$

where $\rho(0)$ is the spectral density at zero in a pure gauge ensemble.

A two flavor theory has a flavor $SU(2)_V \times SU(2)_A \cong O(4)$ symmetry. Consider the (real) $O(4)$ vector made up of

$$\vec{\phi} = (\pi^a = i \sum_{ij} \bar{\psi}_i(x) \gamma_5 \tau_{ij}^a \psi_j(x), f_0 = \sum_i \bar{\psi}_i(x) \psi_i(x)) \quad (15)$$

where f_0 is also known as σ , and the opposite parity (real) $O(4)$ vector made up of

$$\vec{\tilde{\phi}} = (a_0^a = - \sum_{ij} \bar{\psi}_i(x) \tau_{ij}^a \psi_j(x), \eta = i \sum_i \bar{\psi}_i(x) \gamma_5 \psi_i(x)) . \quad (16)$$

Here τ^a , $a = 1, 2, 3$, are the $SU(2)$ generators. All eight components are invariant under a global $U(1)$ rotation associated with fermion number. Under a vector $SU(2)$ flavor rotation, the π^a rotate among themselves, the a_0^a rotate among themselves, and f_0 and η are left invariant. Under an axial $SU(2)$ flavor rotation, the π^a mix with f_0 and the a_0^a mix with η . Finally, under a global $U(1)$ axial rotation, $\vec{\phi}$ mixes with $\vec{\tilde{\phi}}$.

Consider the space averaged pion propagator

$$\chi_\pi = \sum_{x,y} \frac{1}{V} \langle \pi^a(x) \pi^a(y) \rangle = \frac{2}{V} \langle \text{Tr}(\gamma_5 \tilde{D})^{-2} \rangle . \quad (17)$$

$(\gamma_5 \tilde{D})^{-2}$ is diagonal in the chiral basis. There are $|Q|$ eigenvalues equal to $\frac{1}{\mu^2}$ and $|Q|$ zero eigenvalues from the global topology. The non-zero eigenvalues appear in multiples of two and are equal to $(1 - \lambda_i^2) / (\lambda_i^2(1 - \mu^2) + \mu^2)$ which is nothing but the diagonal entries of $\frac{1}{\mu} \tilde{D}^{-1}$. Relation (4) in section I therefore follows. We also obtain

$$\begin{aligned} \frac{1}{V} \text{Tr}(\gamma_5 \tilde{D})^{-2} &= \frac{|Q|}{\mu^2 V} + \frac{1}{V} \sum_i \frac{2(1 - \lambda_i^2)}{\lambda_i^2(1 - \mu^2) + \mu^2} \\ &= \frac{1}{\mu} \langle \bar{\psi} \psi \rangle_A . \end{aligned} \quad (18)$$

Therefore, we find the relation

$$\chi_\pi = \sum_{x,y} \frac{1}{V} \langle \pi^a(x) \pi^a(y) \rangle = \frac{2}{\mu} \langle \bar{\psi} \psi \rangle . \quad (19)$$

We note that this relation holds for any volume and μ , configuration by configuration. In fact, from (4) it follows that the relation holds for any chiral random source that might be used for stochastic estimates of χ_π and $\langle\bar{\psi}\psi\rangle$.

Using, similarly,

$$\frac{1}{V}\text{Tr}(\tilde{D}^{-2}) = \frac{|Q|}{\mu^2 V} + \frac{1}{V} \sum_i \frac{2(1 - \lambda_i^2) [\mu^2(1 - \lambda_i^2) - \lambda_i^2]}{[\lambda_i^2(1 - \mu^2) + \mu^2]^2} \quad (20)$$

we find for the space averaged a_0 propagator

$$\chi_{a_0} = \sum_{x,y} \frac{1}{V} \langle a_0^a(x) a_0^a(y) \rangle = -\frac{2}{V} \langle \text{Tr} \tilde{D}^{-2} \rangle = 2 \left\langle \frac{d}{d\mu} \langle \bar{\psi}\psi \rangle_A \right\rangle. \quad (21)$$

For the space averaged f_0 propagator we find

$$\chi_{f_0} = \sum_{x,y} \frac{1}{V} \langle f_0(x) f_0(y) \rangle = \frac{4}{V} \langle [\text{Tr} \tilde{D}^{-1}]^2 \rangle - \frac{2}{V} \langle \text{Tr} \tilde{D}^{-2} \rangle, \quad (22)$$

and for the space averaged η propagator

$$\chi_\eta = \sum_{x,y} \frac{1}{V} \langle \eta(x) \eta(y) \rangle = \frac{2}{V} \langle \text{Tr}(\gamma_5 \tilde{D})^{-2} \rangle - \frac{4}{V} \langle [\text{Tr}(\gamma_5 \tilde{D})^{-1}]^2 \rangle. \quad (23)$$

To discuss these chiral susceptibilities, we again distinguish four cases:

- We consider full QCD in a finite volume and recall that gauge fields with non-zero topology are suppressed by $\mu^{2|Q|}$, while gauge fields with accidental zeromodes are suppressed by $\mu^{4n'_z}$ from the fermion determinant. Using eqs. (18), (20) and (9) we find

$$\chi_\eta - \chi_{a_0} = \frac{8}{V} \left\langle \sum_i \frac{\mu^2(1 - \lambda_i^2)^2}{[\lambda_i^2(1 - \mu^2) + \mu^2]^2} \right\rangle + \frac{4\langle|Q|\rangle}{\mu^2 V} - \frac{4\langle Q^2 \rangle}{\mu^2 V}. \quad (24)$$

Taking the $\mu \rightarrow 0$ limit, the first term on the right hand side vanishes, while for the others only the sectors with $Q = \pm 1$ contribute, for which the two remaining terms cancel. Therefore we obtain

$$\lim_{\mu \rightarrow 0} (\chi_\eta - \chi_{a_0}) = 0, \quad (25)$$

and, as expected in a finite volume, the $O(4)$ symmetry is unbroken in the massless limit. On the other hand, consider

$$\begin{aligned}
\omega &= \chi_\pi - \chi_{a_0} = \frac{2}{\mu} \langle \bar{\psi} \psi \rangle - 2 \left\langle \frac{d}{d\mu} \langle \bar{\psi} \psi \rangle_A \right\rangle \\
&= \frac{8}{V} \left\langle \sum_i \frac{\mu^2 (1 - \lambda_i^2)^2}{[\lambda_i^2 (1 - \mu^2) + \mu^2]^2} \right\rangle + \frac{4 \langle |Q| \rangle}{\mu^2 V} \\
&= \chi_\eta - \chi_{a_0} + \frac{4 \langle Q^2 \rangle}{\mu^2 V} .
\end{aligned} \tag{26}$$

We have used (19) and (21) in the first line, (18) and (20) in the second line and (24) in the last line. Since $\chi_\eta - \chi_{a_0}$ vanishes in the massless limit, we obtain

$$\lim_{\mu \rightarrow 0} \omega = \lim_{\mu \rightarrow 0} \frac{4 \langle Q^2 \rangle}{\mu^2 V} . \tag{27}$$

The $U(1)_A$ symmetry, therefore, remains broken in a finite volume, due to topology. Only the sectors with $Q = \pm 1$ contribute in the massless limit, giving a finite result. In fact, the four fermi operator making up $\chi_\pi - \chi_{a_0}$ written explicitly in terms of left and right handed spinors, is nothing but the t'Hooft vertex.

- We consider full QCD in the infinite volume limit, taking the volume to infinity first. Then, one expects the $O(4)$ symmetry to be broken down to $O(3) \cong SU(2)$, where the pions are the Goldstone bosons associated with the spontaneous symmetry breaking. Eq. (19) is consistent with this expectation, implying that $m_\pi^2 \propto \mu$. The η , on the other hand, is expected to remain massive due to the axial $U(1)$ anomaly. Therefore we find, using (23), (18) and (9),

$$\begin{aligned}
0 &= \lim_{\mu \rightarrow 0} \lim_{V \rightarrow \infty} \mu \chi_\eta = \lim_{\mu \rightarrow 0} \lim_{V \rightarrow \infty} \frac{\mu}{V} \sum_{x,y} \langle \eta(x) \eta(y) \rangle \\
&= \lim_{\mu \rightarrow 0} \lim_{V \rightarrow \infty} \left\{ 2 \langle \bar{\psi} \psi \rangle - \frac{4 \langle Q^2 \rangle}{\mu V} \right\} ,
\end{aligned} \tag{28}$$

which leads to the relation

$$\lim_{\mu \rightarrow 0} \lim_{V \rightarrow \infty} \frac{2 \langle Q^2 \rangle}{\mu V} = \lim_{\mu \rightarrow 0} \lim_{V \rightarrow \infty} \langle \bar{\psi} \psi \rangle , \tag{29}$$

a relation that has been derived before in the continuum [10].

- We consider a quenched theory in a fixed finite volume, assuming two flavors of valence fermions. Now, gauge fields with non-zero topology are not suppressed, and we obtain from (24) for $\chi_\eta - \chi_{a_0}$ in the massless limit:

$$\lim_{\mu \rightarrow 0} (\chi_\eta - \chi_{a_0}) = \lim_{\mu \rightarrow 0} \frac{4}{\mu^2 V} \langle |Q| + 2n'_z - Q^2 \rangle . \quad (30)$$

Though we expect $\langle n'_z \rangle = 0$ for the number of accidental paired zero modes, we find not only that the O(4) symmetry remains broken in the massless quenched theory in a finite volume, but that $\chi_\eta - \chi_{a_0}$ diverges in the massless limit, unless we restrict the quenched theory to the gauge field sector that has $|Q| = 0, 1$. With this restriction, one can still see the global U(1) anomaly; however, ω diverges as $4\langle |Q| \rangle / (\mu^2 V)$ in the massless limit.

- We consider a quenched theory in the infinite volume limit, taking the volume to infinity before taking the mass to zero. From (17) and (19) it is clear that

$$\chi_\pi - \chi_\eta = \left\langle \frac{4Q^2}{\mu^2 V} \right\rangle . \quad (31)$$

If we restrict ourselves to the topologically trivial sector π and η will be degenerate. If we allow all topological sectors, the right hand side of the above equation will diverge in the massless limit and the η particle will not be well defined (χ_η will become negative).

III. NUMERICAL DETAILS

The main quantity that needs to be computed numerically is the fermion propagator \tilde{D}^{-1} . Certain properties of the Overlap-Dirac operator enable us to compute the propagator for several fermion masses at one time using the multiple Krylov space solver [11] and also go directly to the massless limit. Our numerical procedure to compute the fermion bilinear in (10) and ω in (26) proceeds as follows.

- We note that

$$H_o^2(\mu) = D^\dagger(\mu)D(\mu) = D(\mu)D^\dagger(\mu) = (1 - \mu^2) \left[H_o^2(0) + \frac{\mu^2}{1 - \mu^2} \right] \quad (32)$$

with

$$H_o^2(0) = \frac{1}{2} + \frac{1}{4} [\gamma_5 \epsilon(H_w) + \epsilon(H_w) \gamma_5] \quad (33)$$

- Eq. (32) implies that we can solve the set of equations $H_o^2(\mu)\eta(\mu) = b$ for several masses, μ , simultaneously (for the same right hand b) using the multiple Krylov space solver described in Ref. [11]. We will refer to this as the outer conjugate gradient inversion.
- It is now easy to see that $[H_o^2(\mu), \gamma_5] = 0$, implying that one can work with the source b and solutions $\eta(\mu)$ restricted to one chiral sector.
- The numerically expensive part of the Overlap-Dirac operator is the action of $H_o^2(0)$ on a vector since it involves the action of $[\gamma_5 \epsilon(H_w) + \epsilon(H_w) \gamma_5]$ on a vector. If the vector b is chiral (*i.e.* $\gamma_5 b = \pm b$) then, $[\gamma_5 \epsilon(H_w) + \epsilon(H_w) \gamma_5] b = [\gamma_5 \pm 1] \epsilon(H_w) b$. Therefore we only need to compute the action of $\epsilon(H_w)$ on a single vector.
- In order to compute the action of $\epsilon(H_w)$ on a vector one needs a representation of the operator $\epsilon(H_w)$. For this purpose we use the optimal rational approximation for $\epsilon(H_w)$ described in Ref. [6]. As described in [6], the action of $\epsilon(H_w)$ in the optimal rational approximation amounts to solving equations of the form $(H_w^2 + q_k)\eta_k = b$ for several k which again can be done efficiently using the multiple Krylov solver [11]. We will refer to this as the inner conjugate gradient inversion.
- A further improvement can be made by projecting out a few low lying eigenvectors of H_w before the action of $\epsilon(H_w)$. The low lying eigenvectors can be computed using the Ritz functional [12]. This effectively reduces the condition number of H_w and speeds up the solution of $(H_w^2 + q_k)\eta_k = b$. In addition the low lying subspace of H_w is treated exactly in the action of $\epsilon(H_w)$ thereby improving the approximation used for $\epsilon(H_w)$.

- Since in practice it is the action of $H_o^2(\mu)$ on a vector we need, we can check for the convergence of the complete operator at each inner iteration of $\epsilon(H_w)$. This saves some small amount of work at $\mu = 0$ and more and more as μ increases, while at $\mu = 1$ (corresponding to infinitely heavy fermions) no work at all is required.

We stochastically estimate $\text{Tr}\tilde{D}^{-1}$, $\text{Tr}(\gamma_5\tilde{D})^{-2}$ and $\text{Tr}\tilde{D}^{-2}$ in a fixed gauge field background. To be able to do this efficiently, and in order to compute this at arbitrarily small fermion masses, we first compute the low lying spectrum of $\gamma_5 D(0)$ using the Ritz functional method [12]. This gives us, in particular, information about the number of zero modes and their chirality.² In gauge fields with zero modes we always find that all $|Q|$ zero modes have the same chirality. We have not found any accidental zero mode pairs with opposite chiralities. We then stochastically estimate the three traces above in the chiral sector that does not have any zero modes. In this sector, the propagator with any source is non-singular even for zero fermion mass. Given a Gaussian random source b with a definite chirality we solve the equation $H_o(\mu)^2\eta(\mu) = b$ for several values of μ . Then we compute $(1 - \mu)\xi(\mu) = D^\dagger(\mu)\eta(\mu) - b$. The stochastic estimate of $\text{Tr}\tilde{D}^{-1}$ is obtained by computing $b^\dagger\xi(\mu)$ and averaging over several independent Gaussian chiral vectors b . The stochastic estimate of $\text{Tr}(\gamma_5\tilde{D})^{-2}$ is similarly obtained by computing $\xi^\dagger(\mu)\xi(\mu)$ and averaging over several independent Gaussian chiral vectors b . To estimate $\text{Tr}\tilde{D}^{-2}$ we also compute $(1 - \mu)\xi'(\mu) = D(\mu)\eta(\mu) - b$. Then $\text{Tr}\tilde{D}^{-2}$ is stochastically obtained by computing $\xi'^\dagger(\mu)\xi(\mu)$ and averaging over several independent Gaussian chiral vectors b . Since the stochastic estimates were done in the chiral sector that does not contain any zero modes, the result has to be doubled to account for the contributions from the non-zero modes in both chiral sectors. The contributions from the zero modes due to topology, finally, are added on analytically from the appropriate equations in section II. Since modes with $\lambda_i^2 = 1$ do not contribute at

²The topology and chirality information can also be obtained from the spectral flow method of H_w [13].

all to \tilde{D}^{-1} , we do not have to worry about double counting these edge modes.

IV. NUMERICAL RESULTS

For our numerical simulations, we used the usual hermitian Wilson–Dirac operator $H(m) = \gamma_5 W_w(-m)$ with a negative fermion mass term [1] at $m = 1.65$. Our main results are for quenched $SU(3)$ $\beta = 5.85$, where we have three volumes, and $\beta = 5.7$, where we considered one. In Table I, we show the simulation parameters and number of configurations used. From our previous work with the spectral flow of the hermitian Wilson–Dirac operator [13], we have higher statistics estimates of $\langle |Q| \rangle$ and $\langle Q^2 \rangle$ which we quote in Table I with N_{top} configurations used. For our stochastic estimates of the various traces, we used N_{conf} configurations and 5 stochastic Gaussian random sources. We found 5 sources to be sufficient. For the plots of $\langle \bar{\psi}\psi \rangle / \mu$ and ω , we used N_{conf} configurations for the topology term with all statistical errors computed using a jackknife procedure.

The fermion masses we used for our simulations range from 0 to 0.5. We note that the number of (outer) conjugate gradient iterations we require is typically about 50, 90, and 200 with a convergence accuracy of 10^{-6} (normalized by the source) for our three volumes (in increasing order) at $\beta = 5.85$. This is consistent with our expectation that while we have chosen a chiral source that has no overlap with the zero modes, the smallest non-zero eigenvalues of $H_o^2(0)$ are decreasing with increasing volume. The number of inner conjugate gradient iterations (used for the application of $\epsilon(H_w)$ on a vector) is about 100, 105, and 150 with a convergence accuracy of 10^{-6} for our three volumes at $\beta = 5.85$. We projected out the 10, 10, and 20 lowest eigenvectors of H_w in the computation of $\epsilon(H_w)$, respectively, before using the optimal rational approximation to compute $\epsilon(H_w)$ in the orthogonal subspace. While costly, the pole method [6,15] of implementing $\epsilon(H_w)$ is clearly the most cost effective in terms of floating point operations compared to other implementations of the Overlap–Dirac operator [6,14],

We show our result for $\langle \bar{\psi}\psi \rangle$ without the topology term included in Figure 1. Shown

(but not discernible) are the results for all four volumes. An expanded view for small mass is shown in Figure 2. For small μ , a linear dependence on μ with zero intercept is expected from Eq. (10). If there is to be a chiral condensate in the infinite volume limit the slope near $\mu = 0$ should increase with volume. To see this effect we show $\langle\bar{\psi}\psi\rangle/\mu$ for all our data sets in Figure 3. For sufficiently small μ , we see linearity in μ due to finite volume effects. This linearity is manifested as a constancy in $\langle\bar{\psi}\psi\rangle/\mu$. As the volume is increased, the mass region where linearity sets in is shifted to smaller values. However, the slope near $\mu = 0$ does not increase proportional to the volume and we conclude that there is no definite evidence for a chiral condensate in the infinite volume limit yet.

We show $\langle\bar{\psi}\psi\rangle$ with the topology term included in Figure 4. As expected from Eq. (10), the topology term diverges in a finite volume for $\mu \rightarrow 0$. However, the singularity is decreasing for increasing volume. For sufficiently large volumes, we expect that the quenched $\langle|Q|\rangle$ scales like \sqrt{V} . From Table I we see that the increase of $\langle|Q|\rangle$ from $8^3 \times 16$ to 8×16^3 is consistent with a \sqrt{V} growth. But this is not the case when we compare the value at $6^3 \times 12$ with the one at $8^3 \times 16$. This is attributed to a finite volume effect present at $6^3 \times 12$ [13].

More insight into the possible onset of spontaneous chiral symmetry breaking can be obtained by studying ω in Eq. (26). If chiral symmetry is broken then ω should diverge as $\frac{1}{\mu}$; otherwise, it should go to zero as μ^2 . Evidence for chiral symmetry breaking in the infinite volume limit should show up as a $\frac{1}{\mu}$ behavior in ω at some moderately small fermion masses (an increase in the value of ω as one decreases the fermion mass) that turns over to a μ^2 behavior at very small fermion masses. We show ω without the topology term added in Figure 5. We see a turnover developing in the $\beta = 5.85$ data as the volume is increased around $\mu \sim 10^{-2}$. The turnover is also present in the data at $\beta = 5.7$. Therefore it is possible that there is an onset of chiral symmetry breaking, but the effect is not strong enough for us to be able to extract a value for the chiral condensate.

When we add the topology term in ω , as shown in Figure 6, the turnover region is completely obscured. This result demonstrates how finite volume effects relevant for a study of chiral symmetry are obscured by topology. To be able to extract the chiral condensate in a

quenched theory from finite volume studies it would therefore be helpful to remove the contribution from topology. This is possible with the Overlap-Dirac operator as demonstrated here.

V. CONCLUSIONS

We have derived the standard continuum relations among various fermionic observables by working on a finite volume lattice with the Overlap-Dirac operator. Our results are general and apply equally well to the Overlap-Dirac operator of Neuberger [1] and domain wall fermions for infinite extent in the extra fifth dimension [4]. These relations do not reveal any new physics but allow us to disentangle the contribution of topology and simplify our numerical simulations. We should emphasize that the relations follow only because Overlap fermions satisfy the usual chiral symmetries at any lattice spacing, not only in the continuum limit.

We have shown that the standard relation between the pion susceptibility and the fermion bilinear (c.f. (19)) is properly reproduced by our implementation of the Overlap-Dirac operator even in the chiral limit. We found that for the volumes studied the chiral condensate in the quenched approximation at small fermion mass is dominated by the contribution from the global topology. While this contribution eventually vanishes in the infinite volume limit, it overpowers any signs for an onset of a non-vanishing condensate for the volumes that we were able to study. Removing this topological contribution, which is possible in our implementation of the Overlap-Dirac operator, enabled us to perform a finite volume analysis of chiral symmetry breaking. Still, our numerical simulations for quenched $SU(3)$ gauge theory do not present strong evidence for a chiral condensate in the infinite volume limit of the quenched theory; however, there is some evidence for the onset of chiral symmetry breaking as the volume is increased.

ACKNOWLEDGMENTS

This research was supported by DOE contracts DE-FG05-85ER250000 and DE-FG05-96ER40979. Computations were performed on the workstation cluster, the CM-2 and the QCDSF at SCRI, and the Xolas computing cluster at MIT's Laboratory for Computing Science. We would like to thank H. Neuberger for discussions.

- [1] H. Neuberger, *Phys. Lett.* **B417** (1998) 141.
- [2] R. Narayanan and H. Neuberger, *Nucl. Phys.* **B443** (1995) 305.
- [3] D.B. Kaplan, *Phys. Lett.* **B288** (1992) 342.
- [4] H. Neuberger, *Phys. Rev.* **D57** (1998) 5417.
- [5] Y. Shamir, *Nucl. Phys.* **B406** (1993) 90; V. Furman and Y. Shamir, *Nucl. Phys.* **B439** (1995) 54.
- [6] R.G. Edwards, U.M. Heller and R. Narayanan, hep-lat/9807017, to appear in Nuclear Physics B.
- [7] H. Neuberger, hep-lat/9808036, hep-lat/9807009.
- [8] P. Chen, N. Christ, G. Fleming, A. Kaehler, C. Malureanu, R. Mawhinney, G. Siegert, C. Sui, P. Vranas and Y. Zhestkov, hep-lat/9811013, hep-lat/9811026.
- [9] T.Banks and A. Casher, *Nucl. Phys.* **B169** (1980) 103.
- [10] H. Leutwyler and A. Smilga, *Phys. Rev.* **D46** (1992) 5607.
- [11] A. Frommer, S. Güsken, T. Lippert, B. Nöckel, K. Schilling, *Int. J. Mod. Phys.* **C6** (1995) 627; B. Jegerlehner, hep-lat/9612014.
- [12] B. Bunk, K. Jansen, M. Lüscher and H. Simma, DESY-Report (September 1994); T.

Kalkreuter and H. Simma, *Comput. Phys. Commun.* **93** (1996) 33.

[13] R.G. Edwards, U.M Heller, R. Narayanan, *Nucl. Phys.* **B535** (1998) 403–422.

[14] A. Borici, hep-lat/9810064.

[15] H. Neuberger, hep-lat/9806025.

β	size	N_{conf}	N_{top}	$\langle Q \rangle$	$\langle Q^2\rangle$
5.85	8×16^3	31	40	2.54 ± 0.35	10.7 ± 3.5
5.85	$8^3 \times 16$	50	200	1.115 ± 0.067	2.13 ± 0.22
5.85	$6^3 \times 12$	97	400	0.268 ± 0.025	0.323 ± 0.037
5.70	$8^3 \times 16$	50	50	1.98 ± 0.23	6.6 ± 1.3

TABLE I. Simulation parameters at $m = 1.65$. The number of configurations N_{conf} was used for the trace estimates, and N_{top} configurations were used for the estimates of $\langle|Q|\rangle$ and $\langle Q^2\rangle$. The spectral flow method of ref. [13] was used for the estimates of $\langle|Q|\rangle$ and $\langle Q^2\rangle$ for all but the first line.

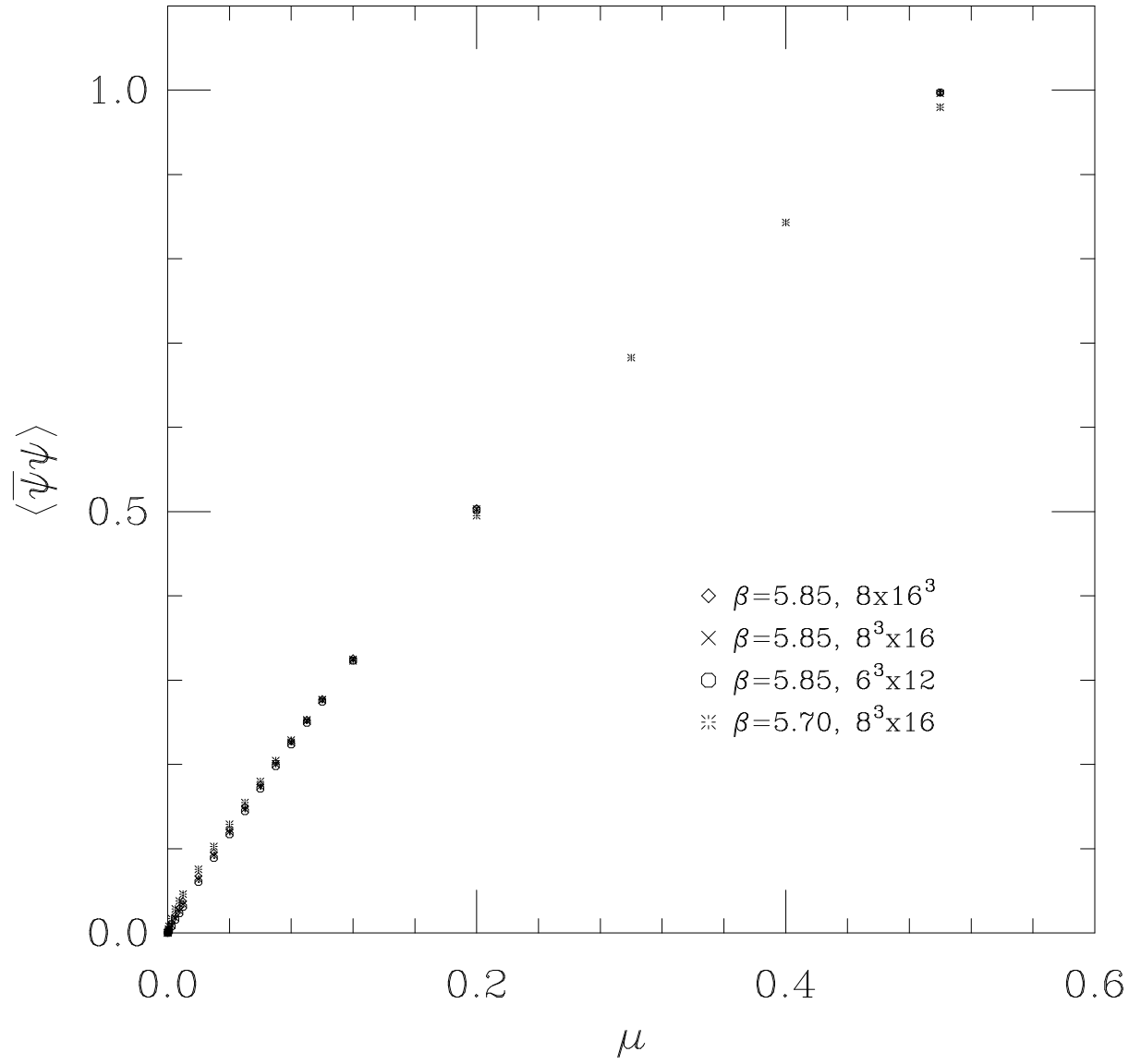


FIG. 1. Plot of $\langle \bar{\psi}\psi \rangle$ without topology for the data sets in Table I.

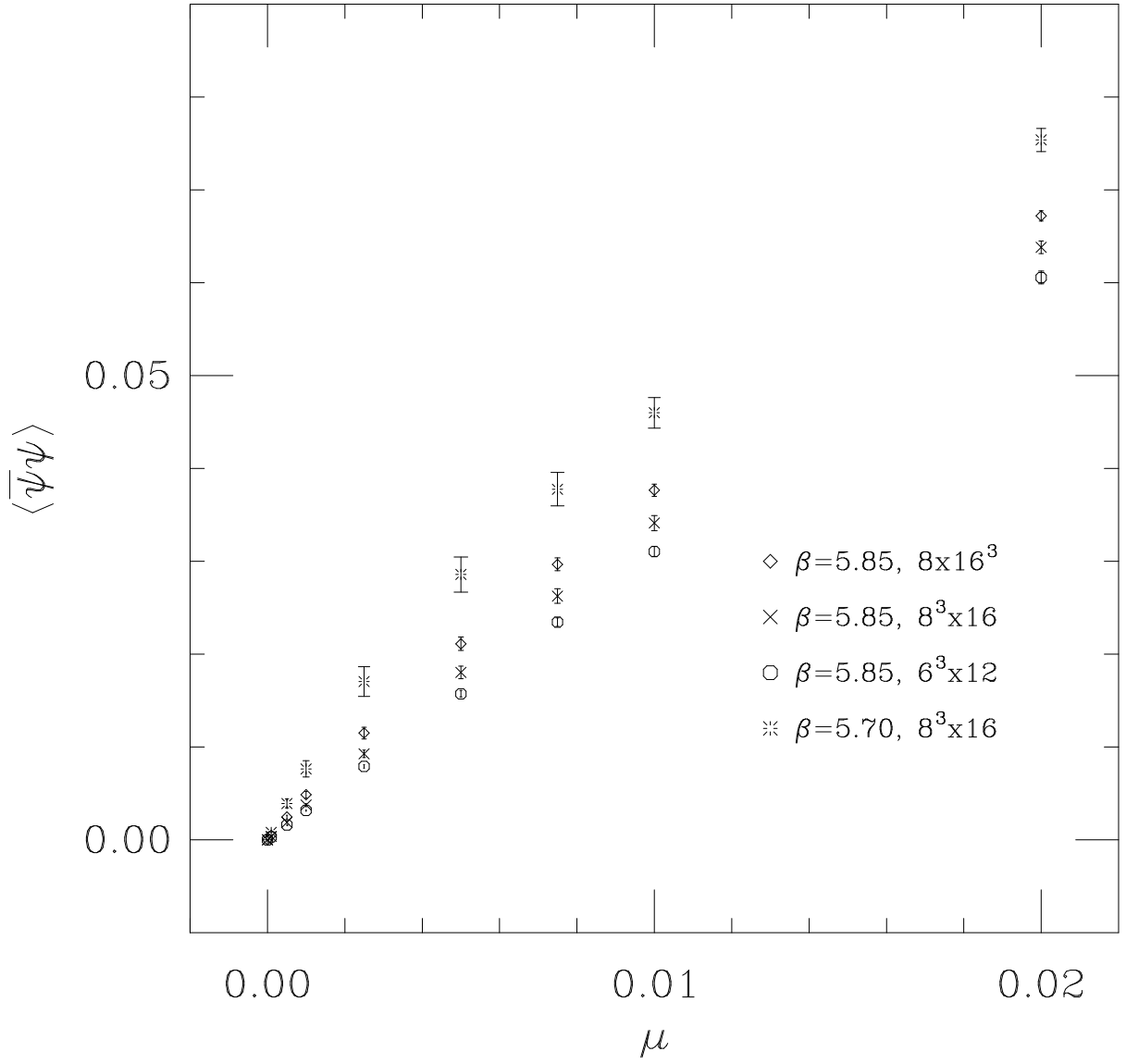


FIG. 2. Expanded view of $\langle \bar{\psi}\psi \rangle$ without topology.

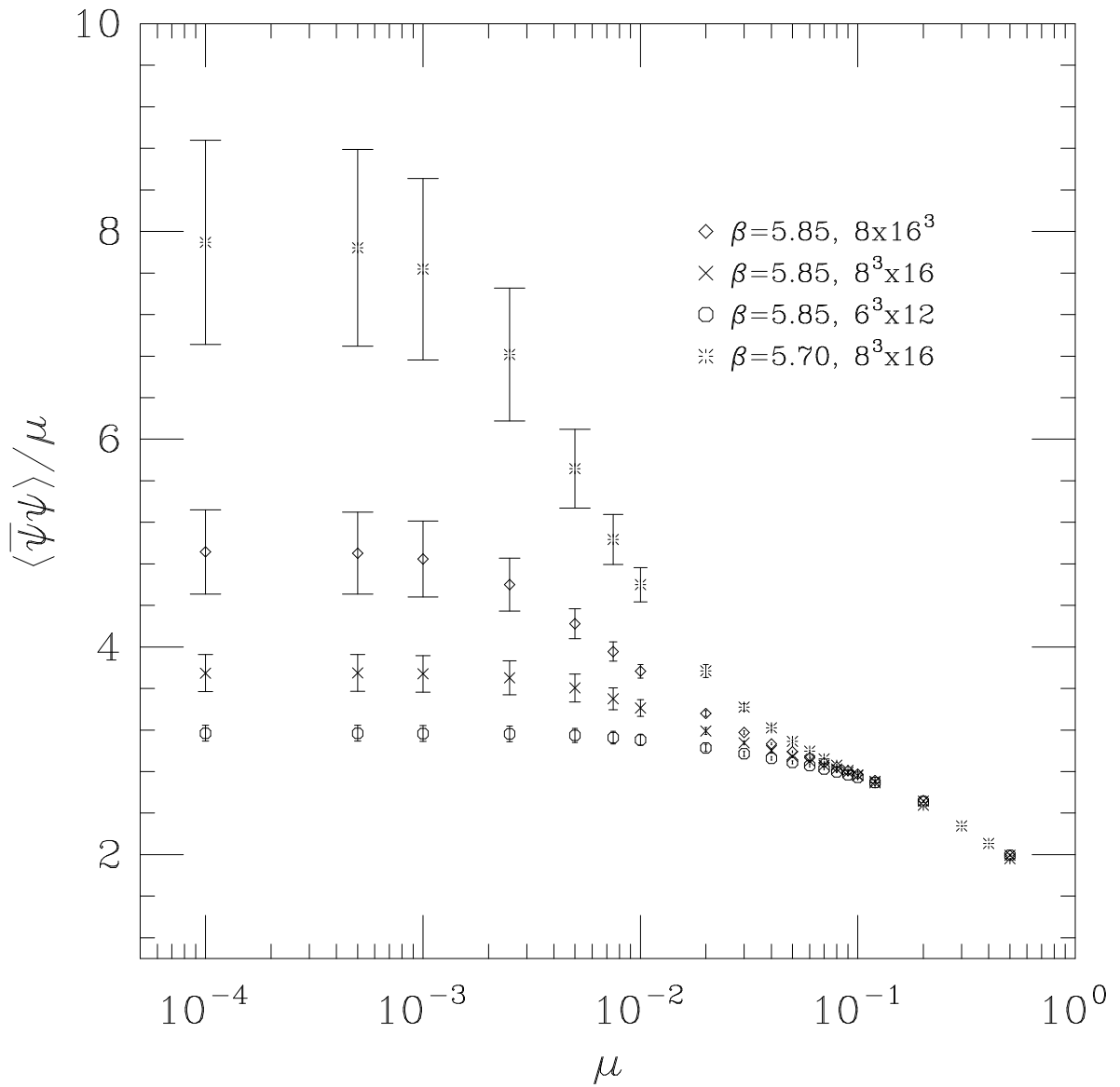


FIG. 3. Plot of $\langle \bar{\psi}\psi \rangle / \mu$ without topology. Strong finite volume effects are manifested as constancy in μ . The mass region where finite volume effects sets in moves to smaller mass values as the volume is increased.

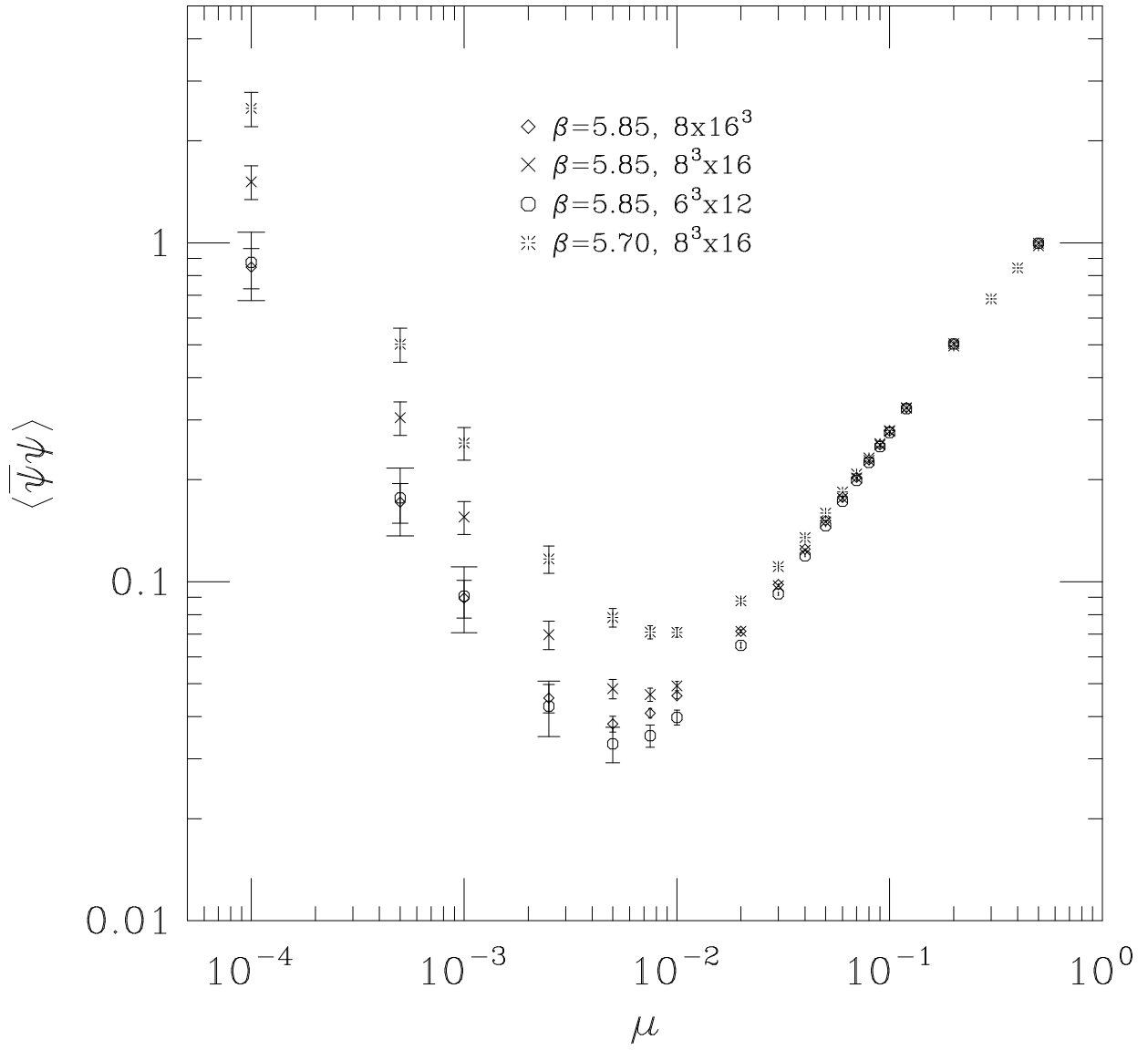


FIG. 4. Plot of $\langle \bar{\psi}\psi \rangle$ with topology.

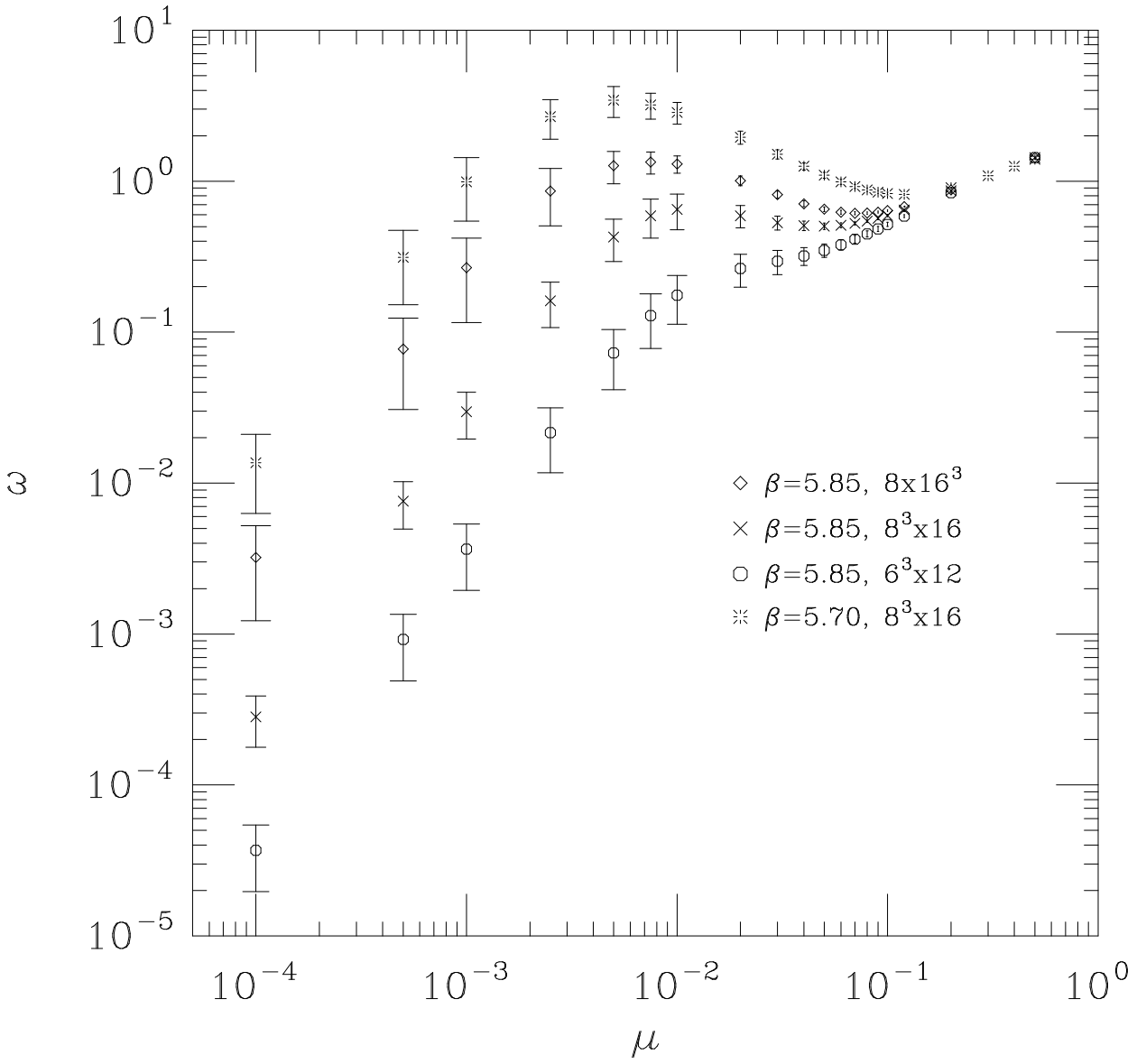


FIG. 5. Plot of ω without topology.

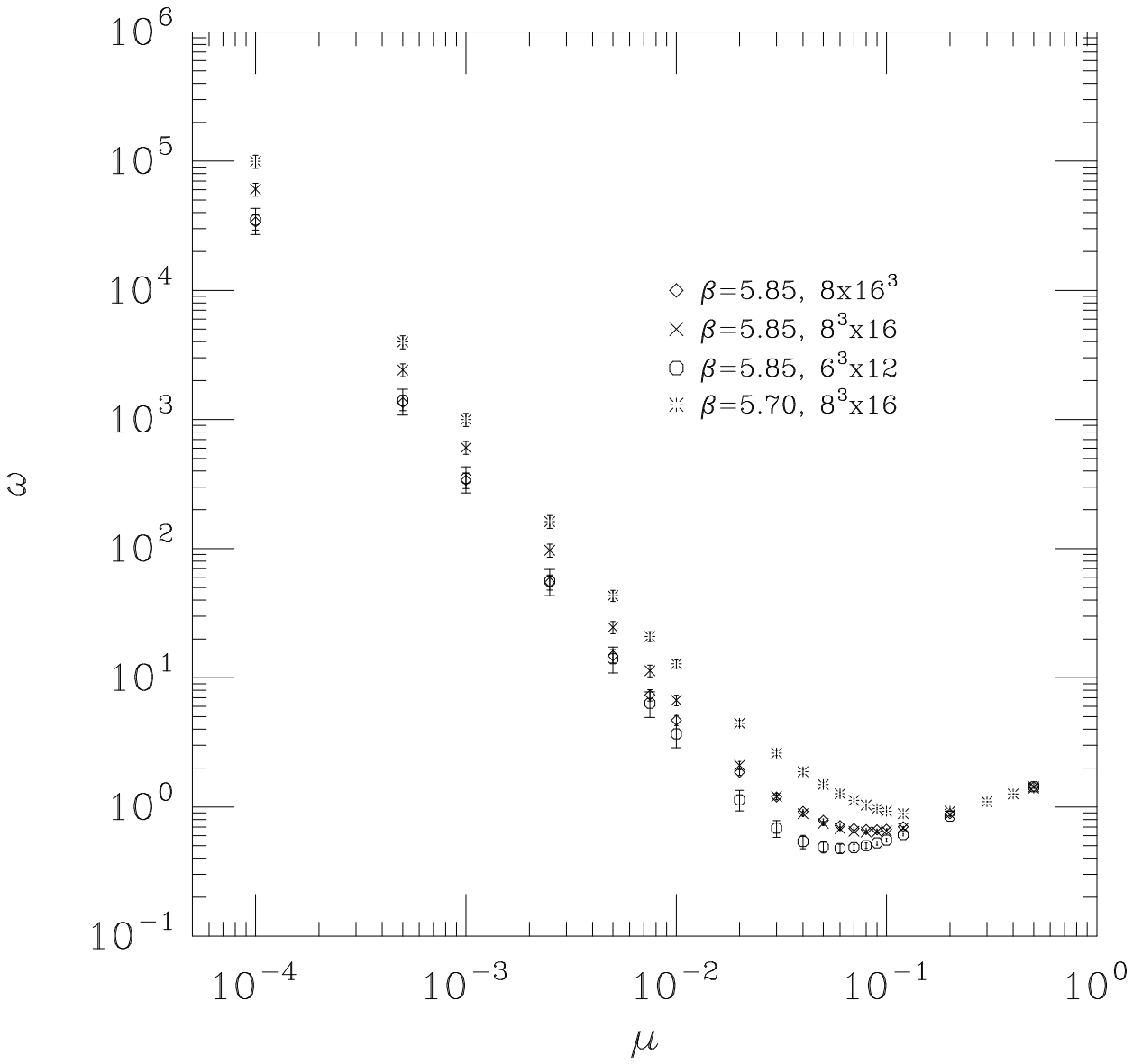


FIG. 6. Plot of ω with topology.